Collisional and thermal effects on liquid lithium sputtering

J. P. Allain,[1,*] M. D. Coventry,[2] and D. N. Ruzic[2]
[1]*Argonne National Laboratory, Argonne, Illinois 60439, USA*
[2]*University of Illinois at Urbana-Champaign, Urbana, Illinois 61801, USA*
(Received 16 December 2006; revised manuscript received 1 July 2007; published 26 November 2007)

The lithium sputtering yield from lithium and tin-lithium surfaces in the liquid state under bombardment by low-energy, singly charged particles as a function of target temperature is measured by using the Ion-surface Interaction Experiment facility. Total erosion exceeds that expected from conventional collisional sputtering after accounting for lithium evaporation for temperatures between 200 and 400 °C. Lithium surfaces treated with high-fluence D atoms are bombarded by H^+, D^+, He^+, and Li^+ at energies between 200 and 1000 eV and 45° incidence. Erosion measurements account for temperature-dependent evaporation. For example, 700 eV He^+ particles bombarding the D-treated liquid Li surface at room temperature result in a sputter yield of 0.12 Li/ion and at temperatures $\sim 2.0T_m$ (where T_m is the melting temperature of the sample), a yield near and above unity. The enhancement of lithium sputtering is observed to be a strong function of temperature and moderately on particle energy. Bombardment of a low-vapor-pressure lithium alloy (0.8 Sn-Li), used for comparison, also results in nonlinear rise of lithium erosion as a function of temperature. Measurements on both pure liquid Li and the alloy indicate a weak dependence with surface temperature of the secondary ion-induced secondary ion emission. Treatment of liquid Li surfaces with D, yields reduced sputtering under He^+ impact by a factor of 5–6 when measured at room temperature due to preferential sputtering effects.

DOI: 10.1103/PhysRevB.76.205434 PACS number(s): 68.49.Sf, 34.50.Dy, 61.25.Mv, 52.40.Hf

I. INTRODUCTION

The temperature dependence of lithium sputtering is important in many applications. These include ion thruster physics, fusion plasma-facing components, extreme ultraviolet lithography, and lithium battery production. Engineering design criteria depend heavily on surface properties such as ion-induced sputtering and the effects of light impurities on the response of the liquid lithium surface to its environment.

From a fundamental point of view, investigating how a surface erodes under energetic particle irradiation as its temperature is increased can aid in our understanding of how atoms in a low-dimensional state (at the surface) evolve under both collisional and thermal mechanisms. This is particularly important for example, at the interface of a liquid-metal and its vapor during energetic ion bombardment.

By convention, collisional sputtering (defined as the number of sputtered atoms per incident bombarding ion) does not have a strong dependence with temperature. This is because the physical sputtering yield of a metal is weakly dependent on surface temperature viz. the weak temperature dependence of the surface cohesion energy. Numerous examples of work in physical sputtering and its dependence on temperature are given in the literature.[1–22] In particular, enhanced erosion mechanisms are observed for heavy-ion, high-energy bombardment leading to dense cascades near the surface with very few cases showing any enhancement correlated to system temperature. In contrast, evaporation does have strong temperature dependence and for a particular material is characterized by its heat of vaporization. In addition here we differentiate between physical sputtering and chemical sputtering. The phenomenon describing lithium emission in this paper is strictly physical sputtering. Chemical sputtering does have strong temperature dependence for certain particle impact energy regimes, however, is not applicable to the system studied here. Furthermore, physical sputtering in the data presented here consists of a collisional and thermal component and these are treated throughout this paper.

The interaction between low-mass energetic charged particles and liquid lithium, from the standpoint of erosion, has received recent attention because of its application as a plasma-facing component (PFC) in fusion devices.[23–28] In addition, the possible use of lithium as an alternative EUV (extreme ultraviolet) radiator in EUV lithography has also attracted interest.[29] Recent experimental results of liquid lithium erosion in the linear plasma device PISCES-B showed enhanced erosion behavior with an increase in target temperature for low-energy deuterium and helium bombardment.[30–32] The enhancement is measured to be substantially greater than erosion by the expected lithium evaporative flux. This phenomenon has been studied in Ion-surface Interaction Experiment IIAX; a particle-beam facility that simulates conditions found in plasma/wall environments of tokamak fusion devices. The enhancement of lithium sputtering with temperature has been measured even with an ion flux 3–4 orders of magnitude lower than that of PISCES-B experiments, for a variety of liquid-metals including Li, Sn, and Sn-Li.

Previous measurements in IIAX included variation of particle energy at oblique incidence under various surface conditions for solid Li (e.g., deuterium-treated and nondeuterium-treated surfaces).[33,34] Oblique ion incidence at 45° with respect to the surface normal simulates conditions at the edge of a tokamak fusion device. In addition, treatment with energetic D particles achieves simulated surfaces saturated with hydrogen isotopes. This is particularly important for lithium because of its high entrapment of hydrogen and, in fact, is one motivator for its application because it would, in principle, lead to low hydrogen isotope recycling and high edge temperature regimes in a tokamak fusion device.[23,27,35] The energy range of incident particles between 200 and

1000 eV in IIAX experiments is carefully selected to simulate expected energies for high edge temperatures characteristic of low-recycling regimes.[36]

At room temperature and just above the Li melting point, previous sputtering measurements in IIAX resulted in little enhancement in lithium erosion.[37] Additional experiments in IIAX and modeling began studying the effect of temperature variation on lithium sputtering at 700 eV with He^+ and 100 eV self-sputtering.[26,38,39] In the present paper, the effect of temperature variation on various states of lithium surfaces (e.g., liquid, segregated layer, deuterated surface) is thoroughly studied. The main observation is as the surface temperature is increased beyond the lithium melting point, nonlinear erosion ensues, even when accounting for evaporation. This paper includes measurements from various light particles H^+, D^+, He^+, and Li^+ exposing Li and Sn-Li samples at 45° incidence with respect to the axis normal to the target. The singly charged ions are accelerated to energies near 200 eV and up to 1000 eV.

Nonlinear sputtering behavior is not expected for the light-mass, low-energy system studied in this work. The sputter yield can be calculated by

$$Y \propto \frac{F_D(x=0)}{NU}, \tag{1}$$

where F_D is the deposited energy distribution at the surface ($x=0$) from particle bombardment in the limit of high-energy (typically energies >100 eV), N is the number density of the target, and U is the surface barrier potential conventionally defined as the material's heat of sublimation as derived by work of Sigmund and Thompson.[12,40,41] The energy deposited into atomic motion leads to the conventional collision cascade. If the collision density or the number of collisions per unit volume is small enough, then the damage process can be described by a simple binary event in which the struck atom is stationary during the collision and the energy deposition, on the average, can be modeled by a linear Boltzmann transport equation by Sigmund.[40] The linear cascade is characterized by the number of defects varying linearly with the total elastic energy deposited and the sputtering yield varying linearly with that part of the deposited energy at the surface.

As the elastic collision cross-section increases with incident ion mass and target mass, a higher recoil density of atoms will result in a higher rate of energy deposition. Eventually, linear cascade assumptions will fail, and a heavily disturbed region or high-density cascade will develop, leading to nonlinear sputtering. This type of nonlinear sputtering is evidenced even at room temperature and is particularly correlated to collisional effects (dense cascades) at high incident particle energies of heavy incident atoms.[9,41,42]

Investigation of lithium erosion presented in this work also includes sputtering measurements from a lithium-tin alloy (0.8 Sn-Li) whose vapor pressure is about three orders in magnitude lower than for pure lithium in the narrow temperature spectrum investigated. This bimetallic system is used as a model system in these nonlinear erosion studies for two primary reasons. First, the system has a very low vapor pressure; thus the evaporation flux is several orders of magnitude lower than sputtering near and above the melting point (melting point for 0.8 Sn-Li is about 320 °C). Therefore, nonlinear erosion processes induced by ion bombardment, if they exist, are more clearly distinguished. Second, the eutectic alloy of Sn-Li has been found to have a Gibbsian-segregated Li surface layer for temperatures studied here at the first 1–2 ML.[43] Since the depth of origin of sputtered particles originates in the top few monolayers,[40] a comparison between liquid 0.8 Sn-Li and liquid Li could provide insight into the underlying mechanisms leading to nonlinear sputtering.

In addition to temperature-dependent erosion measurements, the ion-induced secondary sputtered fraction of lithium and tin-lithium was measured as a function of temperature. The charge state of sputtered species is particularly important for plasma-surface interactions in fusion devices.[44] All surfaces were exposed to a high dose of D particles to simulate conditions in a fusion tokamak environment. Comparison is made to a pure lithium surface to assess the influence of deuterium surface retention on liquid Li sputtering as a function of temperature. Previous studies of solid lithium exposed to deuterium indicated the retention of D atoms on the lithium surface could decrease the absolute lithium sputter yield over 50%.[33,34]

II. EXPERIMENTAL MEASUREMENTS OF LIQUID-METAL EROSION

A. Experimental setup

IIAX has been designed to perform energetic particle-surface interaction studies on liquid metals, such as liquid lithium, liquid tin, and liquid tin-lithium[37,45–47] as shown in Fig. 1. A Colutron ion source is used to create and accelerate gaseous or metal ions onto a 0.066 cm^2 liquid metal target. The bombarding ions are mass selected through an $E \times B$ filter and decelerated near the target by a five-element cylindrical electrostatic lens system. Complete details of the system can be found in earlier papers.[33,37] A 0.75-mm-thick and 100-mm^2 lithium target is inserted in the main chamber containing argon gas at just above an atmosphere. The target can be rotated in order to provide variation in the angle of incidence; for these studies a 45° incidence was applied.

A plasma cup is used to provide *in situ* deuterium plasma cleaning of the target leading to the removal of any oxides or other impurities from the surface. This method also allows for deuterium implantation in lithium (both in solid and liquid states), simulating plasma-facing wall conditions found at the edge of a fusion reactor.[34,37] The irradiated fluence of D atoms in liquid lithium is of the order of 10^{17}–10^{18} D/cm^2, comparable to doses in a tokamak environment. This dose level leads to a concentration ratio of Li:D near unity as measured by Sugai *et al.* and Baldwin *et al.*[48,49] In addition Mirnov *et al.* find using thermal desorption mass spectrometry that the retained D in liquid lithium is released at temperature much lower than that of LiD solute suggesting D can be in solution with lithium in the liquid state.[50]

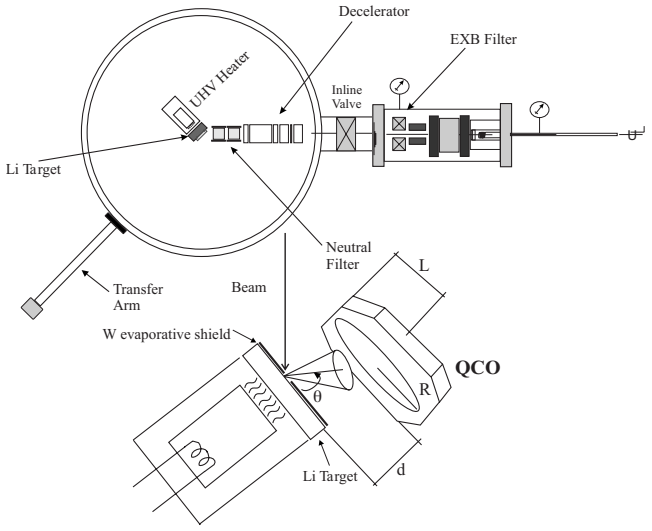

FIG. 1. The ion-surface interaction experiment (IIAX). The experimental device is shown with two differentially pumped chambers: on the right the ion gun chamber, and on the left the main chamber where the lithium target sample is located. The inset diagram shows the position of the QCO (quartz crystal oscillator) with respect to the lithium target. The distance between the lithium target and the QCO is d, the angle of ejected flux ϕ, the radius of the crystal, R and the length from the edge of QCM to center of crystal is designated L.

A dual quartz crystal microbalance dual-crystal unit (QCM-DCU) is rotated in front of the liquid-metal target to collect the sputtered flux, measuring the absolute sputtering yield. This dual QCM technique is described in earlier papers[33,46] and uses one crystal for collection of sputtered material and a reference crystal in thermal contact. The QCM unit is mounted on a manipulator, and thus its spatial and angular position with respect to the target is known. Figure 2 shows a sample trace of the frequency difference Δf of the dual QCM unit against time plotted with ion current on the sample for 700 eV He^+ 45° incidence. Slopes are fitted to the

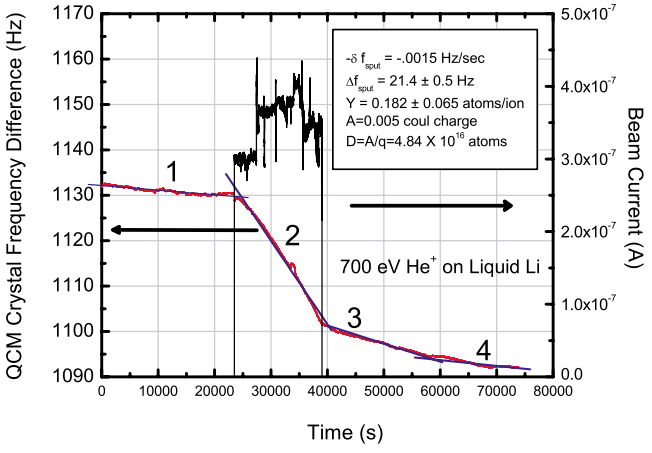

FIG. 2. (Color online) The data show a decrease in the crystal frequency as evaporated lithium is collected. As the liquid sample is exposed to the ion beam, the QCM (quartz crystal microbalance) measures both sputtering and evaporation fluxes.

QCM crystal difference data. The QCM crystal frequency difference in hertz and the beam current on the liquid metal sample in amps are plotted over time. The temporal dependence of the frequency difference has four parts: when the initial signal is measuring evaporation (labeled 1); when the beam is turned on, the signal measures sputtering and evaporation (labeled 2); when the beam is turned off, some oxidation on the QCM crystal as it evaporates (labeled 3); and when the steady-state evaporation signal is reached again (labeled 4). In region 3 we speculate the source of oxidation is ambient water levels and are only detectable here once a fresh sputtered layer on the QCO is deposited.

A small high-temperature, high-vacuum substrate heater is used to heat the target past its melting point to temperatures ranging from 200 to about 400 °C. Measurements of liquid-Li and liquid-Sn-Li sputtering are taken under equilibrium conditions at each target temperature of interest. Therefore, background evaporation is measured before and after ion bombardment at each particular incident energy and surface temperature. A tantalum evaporative shield is floated on top of the liquid metal target. As the sample is heated, a thin oxidized "slag" layer is formed and is removed with an *in situ* mechanical arm. The arm includes a thermocouple, which also measures the temperature of the liquid metal as the arm is partially immersed in the liquid metal during slag removal. Although two thermocouples are utilized to measure the liquid metal temperature, error still exists from the uncertainty of the temperature measurement because heat transfer will occur from the surface of the liquid metal to the stainless steel arm or tantalum shield. Therefore, error bars of the order of 5–7 % are included in the temperature values.

The incident ion flux to the target can range between 10^{13}–10^{14} ions/cm^2/s. The evaporative flux from liquid lithium is 5.1×10^{11} atoms/cm^2/s (at 200 °C) and can reach levels of 10^{13} atoms/cm^2/s or higher at temperatures near 400 °C. The sputtered flux levels vary from 10^{12} and up to 10^{14} Li atoms/cm^2/s. Molecular dynamics calculations have found that the sticking coefficient of thermalized atoms is lower than for sputtered particles with peak energies between 5 and 10 eV (Ref. 44) at temperatures greater than the melting point of lithium. Therefore, the frequency difference temporal slope ($\Delta f/\Delta t$) between evaporated and sputtered fluxes during ion bombardment is measurable.

At temperatures near and above 450 °C, physical sputtering and evaporative fluxes are difficult to discern since the evaporative flux is equal to or greater than the sputtered flux. The partial pressure of impurities in the system is monitored with a quadrupole gas analyzer, and partial pressures of oxygen and hydrocarbons are kept below 10^{-8} Pa. Typical total base pressures before the sample is exposed to the beam are 10^{-6}–10^{-5} Pa. During each lithium-sputtering-yield measurement from liquid Li or liquid Sn-Li samples, the ion-induced secondary ion sputtered fraction (IISIF) is measured. This procedure is done by biasing the sample negatively over a range of voltages and measuring the total ion current. Details of this measurement are included in earlier work.[33] For some IISIF measurements, the liquid Li or liquid Sn-Li surfaces are exposed to identical D plasma doses as those discussed earlier.

B. Data analysis

Analysis of the absolute lithium-sputtering yield from both liquid lithium and liquid tin-lithium samples correlates the time-dependent frequency variation in the crystal signal with the time period of ion beam dose. The calculation of the absolute sputtering yield is then possible after accounting for sputtering of QCM deposited material by incident, highly energetic reflected particles, sticking coefficient of sputtered atoms onto the QCM crystal, and the secondary ion fraction of sputtered atoms. Details of data analysis and calculations are discussed in earlier work using identical QCM-DCU system for both liquid Li and liquid Sn-Li sputtering at temperatures near the melting point.[37,45] A mass balance between the mass loss from the lithium sample and the mass gained on the QCM deposition crystal using the expression

$$M_{\mathrm{QCM}} = \frac{\Delta f}{f} M_{\mathrm{crystal}}, \tag{2}$$

where Δf is the frequency change measured from the raw frequency difference between the deposition and reference crystal data. M_{crystal} is the mass of the crystal given by the manufacturer, and f is the initial frequency of the QCM crystal. The M_{QCM} term incorporates the mass loss due to sputtering from reflected incident particle neutrals from the liquid-metal surface. This results in the expression for the absolute sputtering yield in units of Li atoms/ion:

$$Y = \frac{2N_A}{D f_i S^{\mathrm{QCM}} \Omega m_{\mathrm{Li2O}}} \frac{\Delta f}{f} M_{\mathrm{crystal}} (1 + R_j Y_j^{\mathrm{QCM}} \Omega_j). \tag{3}$$

Y is the absolute sputtering yield in sputtered atoms or particles per ion and D is the total ion dose. Ω is the fraction of the normalized distribution of sputtered particles subtended by the QCM crystal; f_i is a factor accounting for the ion fraction of sputtered species (sputtered secondary ions) ranging from 1.5 to 1.8; and m_{Li2O}, the mass of lithium oxide deposited on the QCM deposition crystal in grams/mol with N_A, is Avogadro's number (6.02×10^{23} atom/mol). A factor of 2 is included because two moles of Li_2O are produced for every four moles of Li consumed. S^{QCM} is the sticking coefficient defined as $1 - R_j^{\mathrm{QCM}}$, where R_j^{QCM} corresponds to the reflection coefficient for sputtered species (sputtered from the target) j off the QCM crystal surface and is calculated by VFTRIM-3D.[51]

Expression (3) does not include the partial sputtering yield of Sn, for the case of Sn-Li sputtering, for two reasons. The sputtering threshold for pure Sn is high near 200–300 eV due to a factor of 2 higher heat of sublimation (3.12 eV) compared to lithium (1.67 eV). At a 45° incidence the sputtering yield of Sn tops 10–20 % at energies of 500–1000 eV, according to simulations with VFTRIM-3D. In addition, XPS measurements show that 99.6% of the mass deposited from sputtered atoms on the QCM crystal is oxidized lithium. These measurements confirm measurements by Bastasz and Whaley of tin-lithium in liquid phase, where lithium atoms segregate to the surface,[43,52] and thus lithium and *not* tin is the ion beam-facing surface. This high level of sputtered lithium from the Sn-Li alloy is also an indication of preferential sputtering of Li consistent with expected Li-to-Sn sputtered ratio.

In addition, beyond the melting point of Sn-Li, the sputtered secondary ion fraction is about 66% (equivalent to pure Li), thus implying that the first few monolayers are made up of pure Li in the liquid Sn-Li alloy eutectic. This result is consistent with measurements of lithium surface segregation in Li-Al and Li-Cu systems conducted by Krauss and Gruen.[53]

III. MODELING OF LIQUID-METAL SPUTTERING

Currently no self-consistent model exists that predicts lithium nonlinear sputtering with temperature. Several models have been developed, including a modified binary collision approximation-(BCA-) based surface model, a hybrid BCA and molecular dynamics model, and a model that accounts for the generation and erosion of adatoms formed on liquid surfaces.[32,38,39,44] Another notable model is the so-called radiation enhanced sublimation (RES) model by Roth and Möller.[54] This model shows increasing sputtering with temperature as evidenced by measurements of carbon bombardment by Ar, He, D, and H. However, this model assumes the source of interstitial and vacancy formation from BCA-based calculations and based on modeling of the liquid lithium surface[39] not adequate for conditions of experiments presented in this paper.

None of these models (excluding RES) have a complete self-consistent picture that explains the mechanism responsible for nonlinear erosion from liquid Li surfaces induced by low-energy, light-particle bombardment as a function of system ambient temperature. In fact, these models fail to provide *a priori* the description of liquid-metal sputtering without use of approximations or fitting to the experimental data they are attempting to predict. This difficulty is primarily due to the seemingly multibody behavior inherent in the erosion of liquid Li induced by low-energy, light-particle bombardment at grazing incidence. In addition, this difficulty is exacerbated by the surface structure developed on liquid-metal surfaces at spatial scales near the sputter depth. Atomistic simulations did, however, elucidate on the possible underlying mechanisms behind the enhanced erosion measured for liquid Li surfaces in this work.[39] This particular work described the intricate role nonbinary collisions of near-surface atoms have on the emitted atoms and correlation to "system" temperature.

Although models designed to simulate temperature-dependent collisional sputtering from liquid-metal surfaces are relatively limited, their use can identify surface mechanisms that could help explain experimental evidence for nonlinear erosion of liquid Li and Sn-Li with increasing temperature. This section presents a semiempirical model that combines collisional and thermal terms of liquid lithium sputtering. The model is based on a localized thermal-spike mechanism described by a localized volume of mobile atoms characterized by low cohesive energy. The semiempirical model is advantageous in that it provides a fast and efficient method to predict liquid-metal sputtering as a function of temperature without the need for computationally expensive

molecular dynamics runs with approximate potentials or approximations of binding energies used in Monte Carlo BCA-based simulation methods.

A. Semiempirical modeling of collisional sputtering

To incorporate the energy dependence of ion-induced sputtering, we use the Bohdnansky-Sigmund-Yamamura (BSY) model for expressing the collisional sputtering yield term

$$Y(E,\theta) = \Lambda F_D(E,\theta,x=0). \tag{4}$$

With the material factor Λ and $F_D(E,\theta,x=0)$ the surface-deposited energy as defined by Jakas.[55] With $F_D(\varepsilon,x=0) = Ns_n^{\mathrm{KrC}}(\varepsilon)\alpha(M2/M1)$ assuming an isotropic cascade and the material factor defined as $\Lambda = 0.042/NU$ with U the surface binding energy. This expression by Sigmund *et al.*[56] is calibrated to experimental data, and appropriate scaling factors are applied, resulting in an empirical relation known as the Bohdansky formula,[40,57] for normal incidence

$$Y(E_0,\theta=0^\circ) = Qs_n^{\mathrm{KrC}}(\varepsilon)\left|1-\left(\frac{E_{\mathrm{th}}}{E_0}\right)^{2/3}\right|\left(1-\frac{E_{\mathrm{th}}}{E_0}\right)^2. \tag{5}$$

In this case Q is known as the yield factor and is expressed as

$$Q = \frac{0.042}{U}\alpha(M2/M1). \tag{6}$$

Here $s_n^{\mathrm{KrC}}(\varepsilon)$ is the nuclear stopping cross-section normalized to the reduced energy ε. The reduced energy is the ratio of E_0 and E_{TF}, where E_{TF} is the energy in the center-of-mass system for a head-on collision with the screening radius as the nearest approach. The factor α is a dimensionless number dependent on the mass ratio M_2/M_1, incident energy, and angle of incidence.[40] Lastly, E_0 is the incident particle energy, U is the surface binding energy, and E_{th} is the threshold energy where the sputtering yield becomes zero.

This empirical relation can be expressed as a function of the angle of incidence. A revised formula, which uses the treatment by Yamamura *et al.*,[58] results in the relation

$$Y_{\mathrm{coll}}(E_0,\theta) = Qs_n^{\mathrm{KrC}}(\varepsilon)\left[1-\left(\frac{E_{\mathrm{th}}}{E_0}\right)^{2/3}\right]\left(1-\frac{E_{\mathrm{th}}}{E_0}\right)^2 \times\frac{1}{(\cos\theta)^f}\exp\left[f\left(1-\frac{1}{\cos\theta}\right)\cos\alpha_{\mathrm{opt}}\right]. \tag{7}$$

Values for f and α_{opt} are used as fitting parameters. A revised approach adapted by Garcia-Rosales *et al.*[57] uses an analytical fit proposed by Yamamura[58] for the value of f. The empirical expression results in a weak function of f with the incident particle energy E_0 for all M_2/M_1 ratios. However, experiments[57] show that f is a strong function of the incident particle energy E_0 for ratios less than $M_2/M_1=6$ down to self-sputtering values. Therefore, empirical fits to these experimental data in the range of $E_0=100-1000$ eV are used for values of f for the combinations of D, He, and Li bombardment of solid lithium.[33] These fits make up the semiempirical model of the collisional erosion term in this paper.

B. Semiempirical modeling of thermal sputtering

Nonlinear sputtering phenomena can be attributed to thermal spike phenomena in the high-energy, heavy-ion bombardment limit. Here we assume we can utilize such models for the case of low sublimation energy materials (e.g., lithium or magnesium) at moderate particle energies and collisional sputtering components after the treatment by Thompson.[41,59] The thermal sputter yield is defined as

$$Y_{\mathrm{th}}(E,\theta,T^*) = \Lambda_{\mathrm{th}}(T^*)F_D(E,\theta,x=0), \tag{8}$$

where $\Lambda_{\mathrm{th}}(T^*)$ is the thermal material factor, and $F_D(E,\theta,x=0)$ the surface-deposited energy as defined earlier. The thermal material factor is related to the quasiequilibrium energy distribution in the induced spike with average energy Θ per atom $f(E_0,\Theta)$ by the energy distribution of recoil atoms $f_r(E_0,\Theta)$ with initial energy E_0 defined as

$$f_r(E_0,\Theta) = \psi\tau N\Omega f(E_0,\Theta)dE_0, \tag{9}$$

where ψ is the recoil particle current, τ is the time constant for the induced spike temperature, and Ω is the slowing-down volume. The average energy per atom also satisfies the condition that $\Theta > U$, where U is the cohesive energy of the system in the spike volume $N\Omega$. The energy distribution is related to the thermal material factor by definition of the sputter yield and emission probability

$$\Lambda_{\mathrm{th}}(\Theta) = \frac{\tau}{4\pi\Theta}\int dE_0 v_0 f(E_0,\Theta)\int d\Omega_0|\cos\theta_O|P(E_0,\theta_0), \tag{10}$$

where $P(E_0,\theta_0)$, is the emission probability and is defined as $P(E_0,\theta_0) = \left(\frac{E_0-U^*}{\cos^2\theta_0}\right)F(\theta)$, where U^* is the thermodynamic sublimation energy at the melting point and $F(\theta)$ is typically a function describing the emission, in this case $F(\theta)=A\cos\theta$ with constant A. The emission probability function includes the concept of a binding force for a recoil atom to be ejected when arriving at the surface with energy E_0 and angle θ_0. The quasiequilibrium energy distribution in the spike is defined as

$$f(E_0,\Theta) = CE^{1/2}\exp\left(\frac{-3E_0}{2\Theta}\right). \tag{11}$$

The average energy per atom is defined as

$$\Theta \approx \frac{\nu(E)}{N\Omega} = \frac{3}{2}k_BT^*. \tag{12}$$

Combining these relations, one derives the thermal material factor as a function of T^*:

$$\Lambda_{\mathrm{th}}(T^*) = \frac{\tau}{\sqrt{\frac{9\pi}{2}Mk_BT^*}}\exp\left(\frac{-U^*}{k_BT^*}\right). \tag{13}$$

Therefore an expression for the thermal sputter yield as a function of the deposition energy distribution at the surface $F_D(x=0)$ and T^* is obtained.

Given $F_D(E,\theta,x=0)=\alpha(M2/M1)f(\theta)NS_n(E)$, where $f(\theta)$ is the angular dependence for scattered and recoil particles

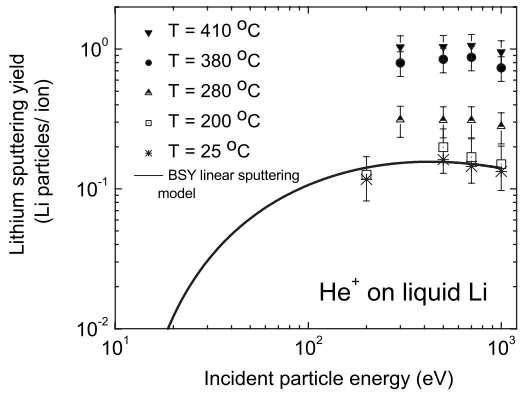

FIG. 3. Measurements of the sputtering yield of lithium bombarded by He^+ ions at 45° incidence for a variety of incident particle energies and target temperatures by Allain *et al.* (Ref. 26). The data is plotted with the BSY (Bohdansky-Sigmund-Yamamura) model based on linear sputtering theory. At each incident particle energy the nonlinear behavior of the lithium-sputtering yield is shown as the temperature increases.

expanded in terms of Legendre polynomials whose expression can be found in the literature.[40] Therefore we get

$$Y_{\mathrm{th}}(E,T^*,\theta) = \frac{\alpha(M2/M1)f(\theta)\tau NS_n(E)}{\sqrt{\frac{9\pi}{2}M2k_BT^*}} \exp\left(\frac{-U^*}{k_BT^*}\right). \tag{14}$$

$T^*=T+T_S$, with T_s defined as the spike temperature due to nonlinear deposition of energy at the surface at ambient system temperature T.

Semiempirical modeling of sputtering as a function of temperature consists of summing a thermal sputtering term and a collisional sputtering term. This approach was adopted by Thompson *et al.*[41] in describing thermal sputtering mechanisms. Adding both the collisional and thermal sputtering terms according to the Sigmund and Thompson models, we obtain what is defined in this paper as the BSY-thermal model.

$$Y = Y_{coll} + Y_{th}. \tag{15}$$

IV. RESULTS AND DISCUSSION

Presented in this section is the lithium-sputtering yield measured in IIAX from bombardment of various singly charged monoenergetic incident particles on liquid lithium and liquid tin-lithium at 45° incidence. Also presented is data on the ion-induced secondary ion sputtered fraction measured for both liquid lithium and liquid tin-lithium. In addition, we discuss the effect deuterium treatment of liquid lithium samples has on the lithium-sputtering yield varies with temperature.

A. Bombardment by helium

Figure 3 shows the He^+ bombardment of liquid lithium measured as a function of incident particle energy for various temperatures at oblique incidence from previous experiments.[26] Helium is used as a control experiment because chemical effects with the lithium surface are absent and analysis of any measured nonlinear erosion is facilitated. Helium-lithium interaction is also relevant if liquid Li is ever considered for a burning plasma fusion reactor. Experiments in IIAX use relatively low ion flux and fluence believed to be below the threshold for bubble formation stability in liquid lithium.

The linear sputtering yield from the BSY model (without temperature effects) is shown in Fig. 3 for comparison. As the temperature is increased beyond the lithium melting point, the lithium-sputtering yield is enhanced beyond the level predicted by linear sputtering theory. The functional dependence of the lithium-sputtering yield on incident particle energy is not as strong as its dependence on temperature. Vaulin measured a similar functional dependence of the sputtering yield with temperature.[60] In addition, similar liquid Li weak energy dependence response was found for lithium interaction with T-11M tokamak[50] and a strong temperature dependence. The result, shown in Fig. 3 from our 2001 experiments, measured this behavior and is the only experimental confirmation measured in a particle-beam facility of lithium's propensity to sputter anomalously with temperature.

At temperatures near the melting point of lithium (~200 °C), the maximum lithium-sputtering yield is reached for incident particle energies near 500 eV. As the temperature is increased, the maximum shifts to lower energies, although this trend is difficult to confirm because of the lack of ion-beam data at energies below 200–300 eV. However, liquid-lithium sputtering data at 75 and 150 eV in PISCES-B shows magnitudes larger than at the 200–300 eV energies in this work, indicating that perhaps a shift does exist.

Earlier data of sputtered energy distributions by Thompson showed similar behavior for conditions using highly-dense near-surface cascades.[12] The spectrum of energy ejecta typically showed shifts to lower energies and a corresponding increase in magnitude. Recent sputtered energy distribution experimental data from liquid Li surfaces under plasma exposure showed similar shifts of the peak energy.[30] The data in Fig. 3 does not show strong energy dependence at energies above 100 eV since a maximum of the nuclear stopping cross section is reached for each temperature studied. Moreover, the absolute sputter yield increases with temperature, yet its energy dependence remains relatively invariant. This behavior suggests a thermal component could be partly responsible for the observed nonlinear erosion behavior exhibited in Fig. 3. However, measured sputtered energy spectra under lithium enhanced erosion conditions show peak energies between 0.1 and 1.0 eV in the range of 200–400 °C, distinctly large compared to typical thermal emission energies (i.e., 0.025 to 0.1 eV).[30] In Fig. 4 we plot the sputter yield of Li against the sample temperature. We find a nonlinear increase of the sputter yield with temperature with a factor of 2.5 increase over the sputter yield at room temperature. Figure 4 also includes data of the BSY thermal sputtering model presented in Sec. III B. When comparing D-treated vs non-D-treated Li surfaces we find about a 50%

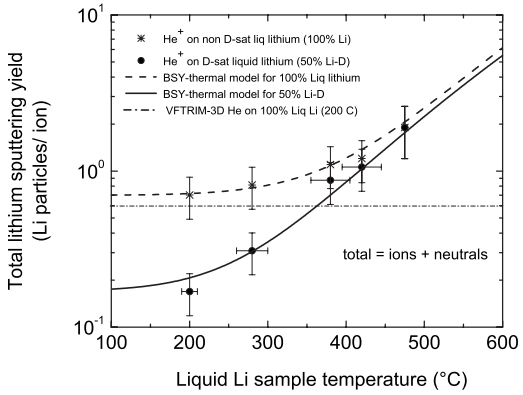

FIG. 4. Lithium sputtering yield as function of sample temperature and deuterium fluence exposure. Also plotted is the BSY-thermal model for deuterium-treated and nondeuterium-treated lithium surfaces.

reduction in the sputtering consistent with solid Li results. However, the effect of D retention as the temperature is increased on the lithium sputter yield competes with nonlinear erosion that begins to dominate at particle energies near 380 °C.

B. Bombardment by hydrogen (H, D)

Bombardment of liquid lithium by hydrogen and deuterium singly charged particles is shown in Figs. 5 and 6. Nonlinear erosion of lithium is again detected. Bombardment with hydrogen and its isotopes is complicated by possible chemical effects between hydrogen and lithium. In addition, since the lithium surface is treated with D-plasma *prior* to ion bombardment, interaction of energetic hydrogen with implanted H particles could lead to complications in data interpretation. Nevertheless, similar results to those with He^+ bombardment have been obtained. A nonlinear erosion rise is obtained at temperatures higher than the melting point of lithium. The energy dependence of lithium sputtering is noticeably weaker than the yield's temperature dependence as shown in Fig. 3 from previous experiments[26] and similar

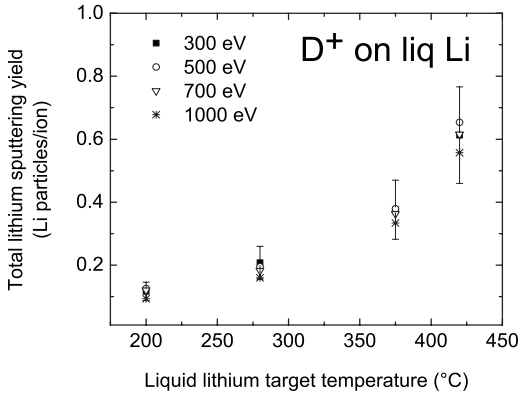

FIG. 5. Measurements of temperature-dependent lithium sputtering from D^+ bombardment for various incident particle energies at 45° incidence of liquid lithium.

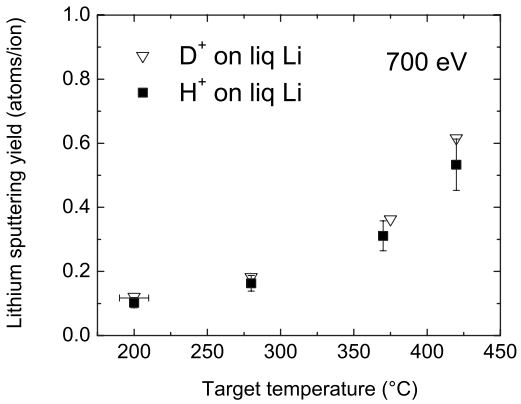

FIG. 6. Lithium-sputtering yield from singly charged deuterium and hydrogen ions on liquid lithium at 700 eV and oblique incidence as a function of target temperature.

behavior under He^+ irradiation. This result indicates that the nonlinear erosion mechanism is not inherently chemical. In addition, although at these fluences no bubble formation of inert implanters is expected (e.g., He), the hydrogen data clearly shows that the nonlinear erosion is not due to bubble formation since hydrogen is highly soluble in liquid lithium. Cases for surface blistering due to hydrogen bombardment have been observed for other materials, but these have thresholds at very high ion fluxes, orders of magnitude higher than the 10^{13}–10^{14} ion/cm^2/s fluxes in these experiments.

Moreover, the measured nonlinear erosion has no isotopic dependence when comparing lithium sputtering results between H and D as shown in Fig. 6. Thus, the lithium erosion enhancement measured must be due to a combination of the local temperature state of the system and the energy imparted by the incident bombarding particle near the surface. Irradiation by H, D, or He is considered light-particle bombardment distinct from conditions found in the generation of highly dense cascades from heavy-ion, high-energy bombardment. In order to compare to a case where the bombarding particle mass is equal or greater than the lithium target, measurements with lithium ions were completed under similar conditions.

C. Liquid lithium self-sputtering

Bombardment by lithium ions is a good case to study and compare with D and He irradiations. In this case we do not expect any stability for bubble formation and in addition we do not expect any strong chemical effects, detectable by IIAX diagnostics. Lithium sputtering from self-bombardment is shown as a function of temperature for various incident Li ion energies in Fig. 7 and as a function of impact energy in Fig. 8 for various temperatures. The enhancement with temperature is also found for lithium self-sputtering as in the case of helium or hydrogen bombardment. This indicates that the underlying mechanism for erosion enhancement with temperature is not due to inert gas bubble formation in the near-surface region followed by microexplosions, since cavity formation and stability would be

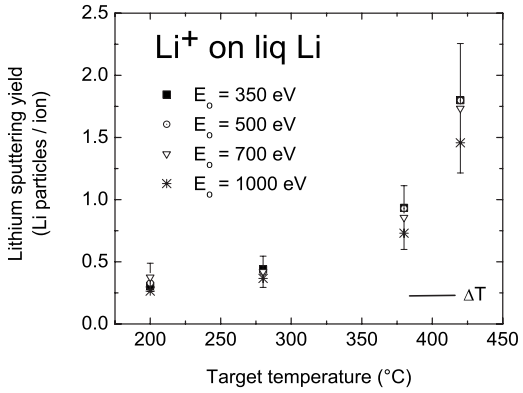

FIG. 7. Measurements of temperature-dependent lithium sputtering from Li^+ bombardment for various incident particle energies at 45° incidence of liquid lithium.

absent when liquid lithium is bombarded by lithium particles. In addition, the enhancement is larger compared to D or He bombardment. This difference indicates that the enhancement is also connected to collision mechanisms and depends on how energy is deposited near the surface (a nonequilibrium process) as opposed to solely a thermally activated process.

Lithium self-bombardment atomistic simulations with molecular dynamics were conducted and demonstrated that the recoil angular and energy distributions played a key role in how energy near the surface is deposited and how this distribution of energy changes with temperature.[39] In addition, the simulations also showed how the binding of sputtered lithium atoms to target atoms just before being emitted behave with temperature. The enhancement of lithium sputtering is also evident when plotting the lithium-sputtering yield against the incident particle energy for various temperatures as shown in Fig. 8. As in the case for D and He bombardment as the temperature of the surface is increased the maximum of the $Y(E)$ curve is shifted to lower energies. This shift again confirms that the underlying mechanisms for enhanced erosion in liquid Li are both thermal and collisional and corroborates low-energy measurements in PISCES-B discussed earlier. In particular the energy of sputtered particles, which for linear collision cascades, follows the Thompson distribution can shift to lower values due to thermally activated mechanisms in systems with low values of U/kT_0, where U is the surface cohesion energy and T_0 is the target temperature.[42] In order to further elucidate on whether the underlying mechanism is purely collisional or thermal or a combination of both, a material with low vapor pressure is chosen for study.

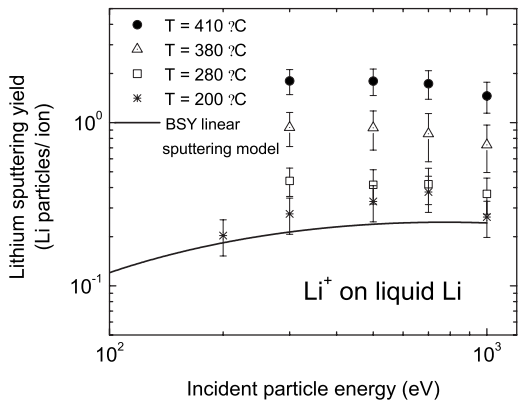

FIG. 8. Measurements of lithium self-sputtering yield as a function of incident particle energy for various temperatures at 45° incidence. Also plotted is the BSY linear sputtering yield model for comparison.

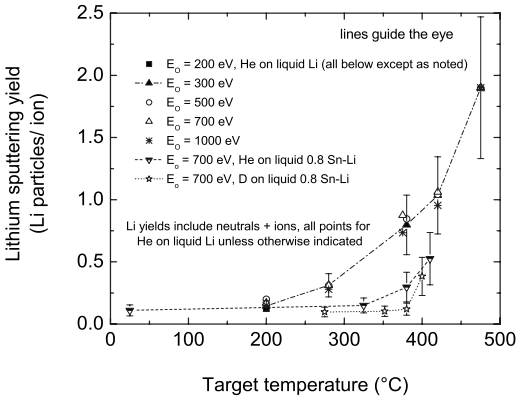

FIG. 9. Lithium sputtering yield from He^+ bombardment on liquid lithium for various incident particle energies and temperatures at oblique incidence. Also shown is the lithium sputtering yield from tin-lithium surfaces from both He^+ and D^+ bombardment.

D. Temperature dependence comparison to liquid SnLi sputtering

The results of lithium-sputtering from both lithium and tin-lithium targets are shown in Fig. 9 for 300–1000 eV He^+ and 700 eV D^+ ions at 45° incidence. In this set of experiments we compare two types of liquid Li surfaces. One the lithium surface after melting has ensued and the other a segregated Li surface layer after melting of the Li-Sn alloy is achieved. The results show an enhancement in the lithium-sputtering yield as the target temperature is increased from the liquid-metal melting point up to temperatures near $2T_m$ for Sn-Li and above $2T_m$ for lithium. The lithium-yield dependence on temperature is stronger than its dependence on the incident particle energy for both types of lithium surfaces. The lithium-sputtering yields from He and D bombardment of tin-lithium targets also show an enhancement, although the threshold for nonlinear sputtering seems to be at a higher target temperature, near 375 °C. Sputtering data indicates that for these temperatures, the vapor pressure of Sn-Li is undetectable by the QCM-DCU diagnostic. In addition, the nonlinear erosion yield shown is not due to any evaporation-related mechanism, thus indicating that nonlinear erosion is possible with light particle bombardment (e.g., He and D at energies <1 keV).

The effect of D implantation on lithium sputtering from liquid Sn-Li surfaces also requires some discussion. From the temperature-dependent sputtering results and XPS data

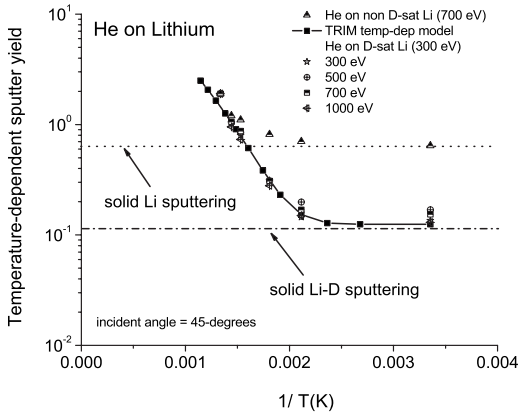

FIG. 10. Inverse-temperature dependence of the lithium sputter yield parametrized with incident particle energy and compared to a TRIM temperature-dependent model (Ref. 38).

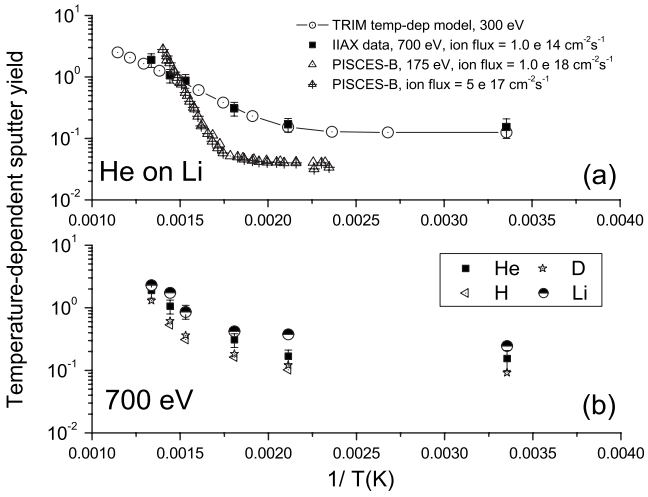

FIG. 11. Inverse-temperature dependence of the lithium sputter yield parametrized with (a) incident particle energy compared to a TRIM temperature-dependent model (Ref. 38) and incident flux, and (b) incident mass.

on the collector crystal, it is evident that lithium is the dominant species during sputtering and that the top few monolayers of liquid Sn-Li are made up mostly of lithium. This is indirect evidence that lithium, being the lower surface tension component at 390 mN/m (525 mN/m for Sn), segregates to the alloy surface in the liquid state viz Gibbsian segregation. This phenomenon was measured with low-energy ion scattering spectroscopy by Bastasz and Whaley for the same temperature range we investigated.[43] However, we find that for Sn-Li in the liquid state, the effect of D exposure does not seem to affect the measured sputter yield of lithium. This may be indirect evidence of low retention levels of hydrogen atoms in bulk Sn-Li surfaces at the liquid state, even though the first few monolayers are pure lithium.

E. Inverse temperature behavior of liquid Li sputtering

Both the thermal behavior and collisional behavior of lithium in the liquid state have been discussed in earlier sections. However, it is insightful to study the inverse-temperature behavior of lithium sputtering as it relates to incident energy, incident mass and incident flux to understand both collisional and thermal contributions to the nonlinear erosion of Li with temperature. Figure 10 shows the inverse-temperature dependence of the lithium sputter yield parametrized with incident particle energy to weigh the collisional vs thermal nature of the enhanced erosion. Figure 11 shows the inverse-temperature dependence of the lithium sputter yield parametrized with incident flux for several energies and incident mass, at 700 eV impact energy. The lithium sputter yield demonstrates an Arrhenius-like behavior at the onset of nonlinear erosion. This is particularly evident when varying the impact energy. Figure 10 also compares the case for a non-D-saturated lithium surface. The onset of nonlinear erosion with temperature is located at nearly the same temperatures, indicating a thermally activated mechanism. In Fig. 11(a) the lithium sputter yield shows two distinct features. One is the onset of nonlinear erosion when comparing impact energies. In this case we compare PISCES-B experimental data of 175 eV He^+ bombardment of liquid Li with an ion flux ranging from $0.5-1.0\times10^{18}$ cm^{-2} s^{-1}. The onset for PISCES-B data is found near 0.00175 1/K and for IIAX data at 700 eV at about 0.00225 1/K. In addition in IIAX, the incident He ion flux ($<10^{14}$ cm^{-2} s^{-1}) is more than four orders of magnitude lower than that used in PISCES-B. As shown in Fig. 11(a), the rate of increase of the lithium sputter yield with temperature is slower by a factor of about 1.44. This enhancement with incident flux may be related to ion-induced near-surface shock waves leading to a higher rate of increase of the lithium sputter yield with temperature. The comparison between IIAX and PISCES-B experimental data is valid even though the impact energies are different, as demonstrated by data from Fig. 10 of the invariance of the lithium temperature-dependent rate increase in yield with impact energy. Figure 11(b) shows that the dependence on incident mass does not change the onset of liquid Li nonlinear erosion with temperature at constant impact energy of 700 eV. This result suggests that thermally activated mechanisms are partly responsible for the nonlinear erosion behavior of liquid Li sputtering. For comparison data from Monte Carlo simulations using an *ad hoc* model in TRIM-SP that accounts for the binding energies varying as a function of temperature is included for 300 eV He bombardment.[38]

F. IISIE vs *T* for D^+, He^+, and Li^+ bombardment of liquid Li and SnLi

The ion-induced secondary ion emission (IISIE) fraction of a metal is known to strongly depend on the chemical state of its surface.[61,62] Previous measurements of solid lithium sputtering by D^+ and He^+ bombardment showed that the IISIE for lithium was 0.66 Li ions/ atom.[33] Basic models exist for estimating the probability of secondary sputtered ions from particle bombardment. These models have been coupled recently with molecular dynamics simulations for

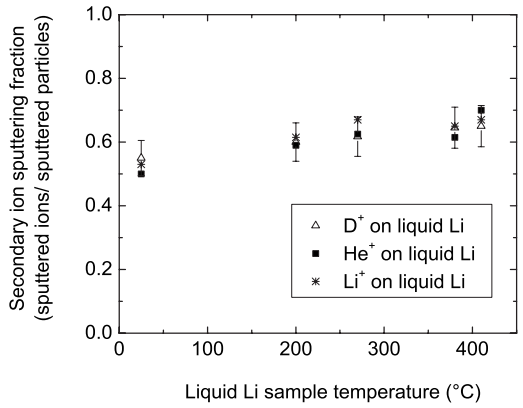

FIG. 12. Measurements of the ion-induced secondary ion sputtering fraction as a function of temperature for 700 eV D^+, He^+, and Li^+ bombardment at 45° incidence on lithium.

the liquid Li system.[44] The models show consistent results of large IISIE for liquid lithium.

Figure 12 shows the result of IIAX experiments for D-treated liquid Li IISIE from 700 eV He^+ bombardment as a function of surface temperature. The IISIE does not show strong temperature dependence and does not depend on the bombarding species. The lack of variation of the IISIE from D^+ bombardment compared to He^+ or Li^+ suggests that for the case of D bombardment the surface electronic properties of liquid Li do not change. This result is important when assessing the role of the IISIE in operation with a liquid Li surface in a fusion reactor. The IISIE will remain high (near 66%) during particle bombardment at an operating temperature range between 200 and 400 °C.

Figure 13 shows results for IISIE from 700 eV He^+ bombardment of liquid Sn-Li as a function of temperature. This experiment clearly indicates, from the standpoint of lithium sputtering, that the nature of the Sn-Li surface dramatically changes as the temperature is raised beyond the melting point of the metal alloy. This is yet additional evidence of Li segregating to the liquid alloy surface, as discussed previously. Moreover, the secondary ion fraction is a phenomenon whose spatial scale is a few monolayers from the surface,

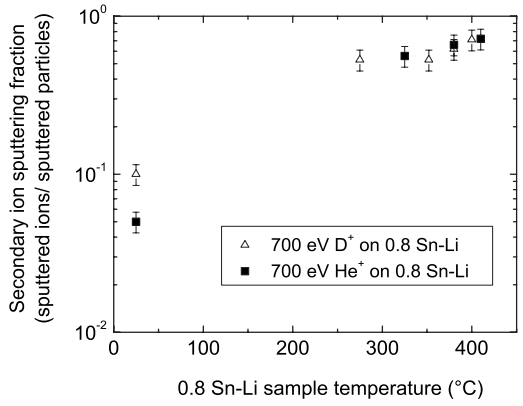

FIG. 13. Measurements of the ion-induced secondary ion sputtering fraction as a function of temperature for 700 eV D^+ and He^+ bombardment at 45° incidence on 0.8 Sn-Li.

and thus the large secondary ion fractions found for temperatures beyond the melting point are not surprising in the context of our data from pure liquid-Li surfaces at similar temperatures. One interesting result from this figure is the solid phase of Sn-Li. There is a measurable difference in secondary ion fraction when bombarding with D^+ compared to He^+. Recall that in both Figs. 12 and 13, the surface is treated with deuterium for fluences corresponding to 1:1 D to Li uptake. For solid phase Sn-Li, however, the secondary ion fractions are quite different from those of D-saturated lithium. The consequence of this is that during D^+ bombardment of Sn-Li, the secondary ion fraction is larger than during He^+ bombardment. This suggests that the secondary ion fraction from Sn-Li may be sensitive to exposure to D^+ compared to He^+ in contrast to results found for pure lithium surfaces. Further work is necessary to clarify this point.

V. CONCLUSIONS

The temperature dependence of lithium sputtering in the liquid state has been investigated in experiments using low-mass charged particles and under self-sputtering. Both thermal and collisional effects are found to be responsible for the enhancement, although thermally activated mechanisms are dominant. The temperature of the system may dictate how cohesive near-surface Li atoms are under particle bombardment. Lithium enhancement was studied by variation of several incident parameters including impact energy, incident mass, and comparisons with incident ion flux. The onset of lithium sputtering enhancement is found to occur at temperatures near 300 °C, and the rate of increase of the yield with temperature is dependent only on incident ion flux and moderately with incident ion mass. The enhancement is not found to be purely collisional. In a purely collisional case the enhancement would be correlated to an increase in the bombardment particle energy as in cases found for heavy-ion nonlinear erosion. However, there is some influence of collisional effects since purely thermal-activated mechanisms would simply lead to thermal-like emission (evaporation).

A semiempirical model developed to predict the temperature-dependent behavior couples both collisional and thermal effects. The thermally activated behavior resembles that of Arrhenius behavior, although this behavior needs to be assessed further. The model assumes a localized damaged region characterized by highly mobile atoms with reduced coordination number at the liquid-vapor interface. The incident ion flux dependence shows that even for about a four-order-of-magnitude difference in ion flux, the rate of increase of the lithium sputter yield with temperature changes at most by 44%. The difference could be due to near-surface localized shock-wave expansion effects. The dependence of the nonlinear erosion with ion flux for these results also suggest that any thermal spikes that exist are too small and too quick that they overlap, which consequently explains the weak dependence of the measured nonlinear Li erosion on impact energy.

All experimental data of temperature-dependent lithium sputtering were taken with mass-loss diagnostic systems not able to discern the species and state (i.e., cluster, molecules)

of sputtered particles. Therefore it is possible that, the enhanced population of sputtered particles could be due to the generation of small clusters during bombardment and shock wave generation, and more prevalent at higher incident ion fluxes. The study of cluster emission from liquid Li surfaces is a topic of future work.

In addition to the study of the temperature dependence of the lithium sputter yield, the secondary ion fraction induced by incident ions was also studied and compared for two material surfaces. A monotonic increase in the secondary ion yield was found with temperature for pure liquid Li. A more pronounced dependence was found when comparing a lithium alloy, 0.8 Sn-Li with a liquid Li surface. In this case once the alloy reached its melting point, a segregated Li layer was formed and the surface behaved similarly to liquid Li as found in the literature using low-energy ion scattering spectroscopy techniques.[43,52]

The effect of deuterium saturation of Li and SnLi surfaces was also studied. Although complete results are not presented, these show that deuterium effectively decreases the absolute sputter yield of Li. Deuterium coverage had some indirect effect on the rate of increase of lithium sputtering after the onset of nonlinear erosion. In this case, some D may be diffusing into the bulk as the temperature is increased during ion bombardment. This effect necessitates further investigation and in particular with atomistic simulations since decoupling from thermally activated mechanisms is very difficult.

ACKNOWLEDGMENTS

The authors would like to thank Dr. Jeffrey N. Brooks and Dr. Ahmed Hassanein for insightful discussions and the referees for valuable feedback. Additional discussions are acknowledged with R. Bastasz, R. Doerner, M. Baldwin, L. Zacharov, R. Majeski, R. Kaita, L.E. Gonzalez, and R. Averback. The skillful work of Matthew Hendricks and Mark Boaz is also acknowledged. This work was supported by the DOE-ALPS program under Grant No. DEFG02-99-ER54515. The submitted manuscript has been created in part by UChicago Argonne, LLC, Operator of Argonne National Laboratory ("Argonne"). Argonne, a U.S. Department of Energy Office of Science laboratory, is operated under Contract No. DE-AC02-06CH11357.

*Present address: Purdue University, W. Lafayette, IN 47907.

[1] H. H. Andersen and H. L. Bay, Radiat. Eff. **19**, 139 (1973).
[2] R. Kelly, Radiat. Eff. **32**, 91 (1977).
[3] R. Kelly, Nucl. Instrum. Methods Phys. Res. B **46**, 441 (1990).
[4] E. M. Bringa and R. E. Johnson, Nucl. Instrum. Methods Phys. Res. B **143**, 513 (1998).
[5] E. M. Bringa, M. Jakas, and R. E. Johnson, Nucl. Instrum. Methods Phys. Res. B **164-165**, 762 (2000).
[6] E. M. Bringa, R. E. Johnson, and L. Dutkiewicz, Nucl. Instrum. Methods Phys. Res. B **152**, 267 (1999).
[7] S. S. Johar and D. A. Thompson, Surf. Sci. **90**, 319 (1979).
[8] D. A. Thompson, J. Appl. Phys. **52**, 982 (1981).
[9] D. A. Thompson, Radiat. Eff. **56**, 105 (1981).
[10] D. A. Thompson and S. S. Johar, Appl. Phys. Lett. **34**, 342 (1979).
[11] M. W. Thompson, Phys. Rep. **69**, 335 (1981).
[12] M. W. Thompson, Philos. Mag. **18**, 377 (1968).
[13] P. Sigmund and M. Szymonski, Appl. Phys. A: Solids Surf. **33**, 141 (1984).
[14] M. Urbassek and P. Sigmund, Appl. Phys. A: Solids Surf. **35**, 19 (1984).
[15] C. Claussen, Nucl. Instrum. Methods Phys. Res. **194**, 567 (1982).
[16] T. Diaz de la Rubia, R. S. Averback, R. Benedek, and W. E. King, Phys. Rev. Lett. **59**, 1930 (1987).
[17] G. H. Vineyard, Radiat. Eff. **29**, 245 (1976).
[18] R. E. Johnson and R. Evatt, Radiat. Eff. **52**, 187 (1980).
[19] R. S. Averback, J. Nucl. Mater. **216**, 49 (1994).
[20] G. S. Chen, Nucl. Instrum. Methods Phys. Res. B **71**, 7 (1992).
[21] P. Sigmund and C. Claussen, J. Appl. Phys. **52**, 990 (1981).
[22] W. O. Hofer, K. Besocke, and B. Stritzker, Appl. Phys. A: Solids Surf. **30**, 83 (1983).
[23] J. N. Brooks, T. D. Rognlien, D. N. Ruzic, and J. P. Allain, J. Nucl. Mater. **290-293**, 185 (2001).
[24] R. F. Mattas (unpublished).
[25] R. F. Mattas *et al.*, Fusion Eng. Des. **49-50**, 127 (2000).
[26] J. P. Allain, M. Nieto, M. D. Coventry, R. Stubbers, and D. N. Ruzic, Fusion Eng. Des. **72**, 93 (2004).
[27] J. N. Brooks, J. P. Allain, R. Bastasz, R. Doerner, A. Hassanein, and R. Kaita, Fusion Sci. Technol. **47**, 669 (2005).
[28] A. Hassanein, J. P. Allain, Z. Insepov, and I. Konkashbaev, Fusion Sci. Technol. **47**, 686 (2005).
[29] V. Banine and R. Moors, J. Phys. D **37**, 3207 (2004).
[30] R. P. Doerner, M. J. Baldwin, R. W. Conn, A. A. Grossman, S. C. Luckhardt, R. Seraydarian, G. R. Tynan, and D. G. Whyte, J. Nucl. Mater. **290-293**, 166 (2001).
[31] R. P. Doerner, M. J. Baldwin, S. I. Krasheninnikov, and D. G. Whyte, J. Nucl. Mater. **313-316**, 385 (2003).
[32] R. P. Doerner, S. I. Krasheninnikov, and K. Schmid, J. Appl. Phys. **95**, 4471 (2004).
[33] J. P. Allain and D. N. Ruzic, Nucl. Fusion **42**, 202 (2002).
[34] J. P. Allain and D. N. Ruzic, in *NATO Science Series: Hydrogen and Helium Recycling at Plasma Facing Materials*, edited by A. Hassanein (Kluwer Academic Publishers, Dordrecht, 2002), Vol. 54, pp. 73.
[35] R. Majeski, R. Doerner, T. Gray, R. Kaita, R. Maingi, D. Mansfield, J. Spaleta, V. Soukhanovskii, J. Timberlake, and L. Zakharov, Phys. Rev. Lett. **97**, 075002 (2006).
[36] J. N. Brooks, J. P. Allain, T. D. Rognlien, and R. Maingi, J. Nucl. Mater. **337-339**, 1053 (2005).
[37] J. P. Allain, D. N. Ruzic, and M. R. Hendricks, J. Nucl. Mater. **290-293**, 180 (2001).
[38] J. P. Allain, M. D. Coventry, and D. N. Ruzic, J. Nucl. Mater. **313-316**, 645 (2003).
[39] J. P. Allain, D. N. Ruzic, M. D. Coventry, D. A. Alman, and M. Nieto, Nucl. Instrum. Methods Phys. Res. B **239**, 347 (2005).
[40] P. Sigmund, Phys. Rev. **184**, 383 (1969).

[41] M. W. Thompson, Vacuum **66**, 99 (2002).
[42] M. W. Thompson, Philos. Trans. R. Soc. London **362**, 5 (2004).
[43] R. Bastasz and J. A. Whaley, J. Nucl. Mater. **72**, 111 (2004).
[44] J. P. Allain, J. N. Brooks, D. A. Alman, and L. E. Gonzalez, J. Nucl. Mater. **337-339**, 94 (2005).
[45] J. P. Allain, D. N. Ruzic, and M. R. Hendricks, J. Nucl. Mater. **290-293**, 33 (2001).
[46] J. P. Allain, in *Department of Nuclear, Plasma and Radiological Engineering* (University of Illinois at Urbana-Champaign, Urbana, 2001), pp. 226.
[47] M. D. Coventry, J. P. Allain, and D. N. Ruzic, J. Nucl. Mater. **313-316**, 640 (2003).
[48] H. Sugai, M. Ohori, and H. Toyoda, Vacuum **47**, 981 (1996).
[49] M. J. Baldwin, R. P. Doerner, S. C. Luckhardt, and R. W. Conn, Nucl. Fusion **42**, 1318 (2002).
[50] S. V. Mirnov, E. A. Azizov, V. A. Evitkhin, and V. B. Lazarev, Plasma Phys. Controlled Fusion **48**, 821 (2006).
[51] D. N. Ruzic, Nucl. Instrum. Methods Phys. Res. B **47**, 118 (1990).
[52] R. Bastasz and W. Eckstein, J. Nucl. Mater. **290-293**, 19 (2001).
[53] A. R. Krauss and D. M. Gruen, J. Nucl. Mater. **85 & 86**, 1179 (1979).
[54] J. Roth and W. Möller, Nucl. Instrum. Methods Phys. Res. B **7/8**, 788 (1985).
[55] M. M. Jakas and D. E. Harrison, Jr., Phys. Rev. Lett. **55**, 1782 (1985).
[56] P. Sigmund, *Sputtering by Particle Bombardment I* (Springer-Verlag, Berlin, 1981).
[57] C. Garcia-Rosales, W. Eckstein, and J. Roth, J. Nucl. Mater. **218**, 8 (1994).
[58] Y. Yamamura, Y. Itikawa, and N. Itoh, IPPJ-AM-26 (Institute of Plasma Physics, Nagoya, Japan, 1983).
[59] M. W. Thompson, Nucl. Instrum. Methods Phys. Res. B **18**, 411 (1987).
[60] E. P. Vaulin, N. E. Georgieva, T. P. Martynenko, and L. V. Feoktistov, Sov. J. Plasma Phys. **7**, 239 (1981).
[61] M. L. Yu, in *Sputtering by Particle Bombardment III*, edited by R. Behrisch and K. Wittmaack (Springer-Verlag, Berlin, 1991), Vol. 64.
[62] R. Brako and D. M. Newns, Surf. Sci. **108**, 253 (1981).